

Jamming of 3D Prolate Granular Materials

K. Desmond and Scott V. Franklin*
Dept. of Physics, Rochester Institute of Technology
(Dated: September 12, 2018)

We have found that the ability of long thin rods to jam into a solid-like state in response to a local perturbation depends upon both the particle aspect ratio and the container size. The dynamic phase diagram in this parameter space reveals a broad transition region separating granular stick-slip and solid-like behavior. In this transition region the pile displays both solid and stick-slip behavior. We measure the force on a small object pulled through the pile, and find the fluctuation spectra to have power law tails with an exponent characteristic of the region. The exponent varies from $\beta = -2$ in the stick-slip region to $\beta = -1$ in the solid region. These values reflect the different origins — granular rearrangements vs. dry friction — of the fluctuations. Finally, the packing fraction shows only a slight dependence on container size, but depends on aspect ratio in a manner predicted by a mean field theory and implies an aspect-ratio independent contact number of $\langle c \rangle = 5.25 \pm 0.03$.

I. INTRODUCTION

Anyone scooping nails from a bin at the hardware store or shoveling hay with a pitchfork has noticed the ability of large aspect-ratio ($\alpha \equiv L/D \gg 1$) granular materials to act as a solid. This state can exist at low packing fractions, raising the possibility of lightweight, rigid building materials. Such materials have practical applications as proppant in oil recovery or conducting networks in quantum dot solar cells. Here we present the first experimental investigation into the dependence of this state on particle aspect ratio and container size.

The jamming of round and low aspect-ratio (< 5) materials has attracted a great deal of recent attention. A canonical example of granular jamming is flow through hoppers, where arches at the exit can support the entire pile [1, 2, 3, 4]. This jammed state, while capable of supporting large constant forces, is not robust when subjected to sharp taps. Indeed, in one set of experiments [4] a jet of air was sufficient to reintroduce flow.

Jamming is also invoked to explain the erratic drag force on an object moving through a granular medium [5, 6]. The object comes to rest when it encounters a connected network of particles that is incapable of rearranging; only when the applied force is large enough to break through this network does the motion begin again. The particles in this network are only a small fraction of the total grains in the pile, those comprising the force chains [7, 8] that terminate on the container walls.

The situation is remarkably different for high aspect-ratio (> 10) granular materials [9]. Philipse [10] noted that particles of aspect ratio larger than 35 emerged as a solid plug when poured. This plug maintained the shape of the original container even in face of external disturbances. This jammed state can therefore be considered both global and robust, the connected network of particles containing a significant fraction of the pile that are incapable of moving around one another. How this solid

like state compares with the jammed state of ordinary granular materials has not yet been explored.

Recent work has investigated the mean drag force exerted by ordinary granular materials on an intruder. Zhou et al. found [11, 12], for example, that mean drag scales linearly with pressure for both mono- and polydisperse materials. Geng and Behringer[13] studied the force fluctuations exerted by a two-dimensional packing of disks and found that the power spectra had a power law tail with exponent -2 , as in three-dimensional systems. Hill et al.[14] and Stone et al.[15, 16] have all looked at plates pushed slowly down into beds of sand, with interesting behaviors as the plate approaches the bottom of the container and a temporal evolution in the granular bed with successive plungings. Finally, Bratberg et al.[17] simulated the quasi-static flow of rigid, frictional disks pushed upward against gravity through a narrow pipe. They observed a transition in the flow when the intruder speed was large.

II. SETUP AND PACKING FRACTION

In our experiments, the force on a small ball pulled upward through a pile of prolate granular materials is measured. Particles are cut from acrylic rods of diameter $d = 1/8''$ or $d = 1/16''$ to varying lengths; aspect ratios vary from 4 to 48. The particles are dropped into cylinders with diameters ranging from $D = 1''$ to $D = 4''$. A dimensionless container diameter is formed by dividing by the particle length ($\tilde{D} \equiv D/L$); the smallest \tilde{D} is 0.67, the largest 12. At the bottom of the pile sits a small ($d = 0.25''$) metal ball connected to string that runs up through the pile. We have confirmed that packings formed around the string have the same packing fraction as those formed in the string's absence. The string is wound around the shaft of a motor that turns with constant angular speed. A force sensor measures the tension in the string to within 0.5% at kHz resolution. For the range of forces in our experiments, the string and force sensor act Hookian with spring constant $k = 1600$ N/m. The motion of the ball can be erratic; when the resis-

*svfspd@rit.edu; <http://piggy.rit.edu/franklin/>

tance of the pile exceeds that applied by the string the ball will stop moving until the applied force, increasing as the string is wound, is again large enough to induce motion.

Particles are simply dropped into the cylinder. “Fluffing” the pile with air, a technique used to prepare ordinary granular materials in a low density state, does not significantly decrease the packing fraction of rods [18]. The packing fraction is plotted (log-log) versus aspect ratio in Fig. 1, with different symbols indicating different dimensionless container sizes. The data from different size containers are reasonably close to one another, except for a few points at the low \tilde{D} . At these values the particles tend to align with the sidewalls, introducing significant orientational correlation and higher packing fractions.

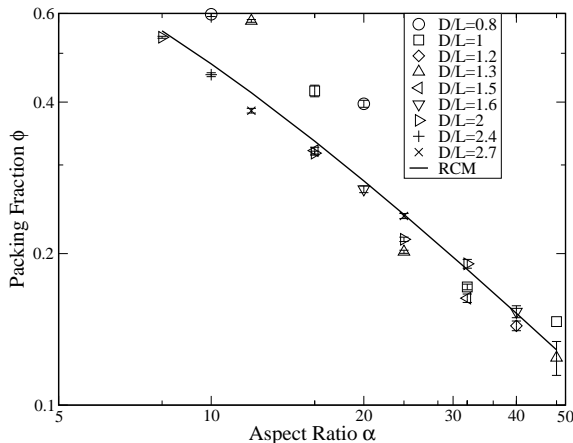


FIG. 1: Log-log plot of packing fraction ϕ as a function of particle aspect ratio α . Data are grouped by constant dimensionless container diameter $\tilde{D} \equiv D/L$. With the exception of a few points at low \tilde{D} (where significant particle alignment occurs), the data are well-fit by a mean-field theory with only one free parameter.

To gain some idea of the randomness of the initial packing we compare the packing fraction with a mean-field theory the *Random Contact Model* (RCM) [10]. The basic assumption of this model is that contacts between particles are uncorrelated, a significant difference from the correlated contacts that result in ordered packing of, for example, disks or rods. If the contacts are uncorrelated, then the packing can be thought of as a collection of independent pairs of rods in contact.

A key finding of Philipse is that the average number of contacts $\langle c \rangle$ scales linearly with the particle concentration. To show this, Philipse begins with the fraction of orientations made inaccessible to a particle by the existence of another particle. This is a function of the center-of-mass separation of the two particles; when two rods are close together, they must be more nearly aligned to prevent overlapping. Earlier work on the packing of rods in two dimensions [9] calculated the functional dependence of the excluded fraction of orientations $f_{\text{ex}}(\vec{r})$

analytically and found that, while both experiment and simulations contained long-range correlations, the functional form was universal over several orders of magnitude in aspect ratio. The average number of contacts is then proportional to the product of the excluded fraction of orientations and the local number density:

$$\langle c \rangle = \frac{1}{2} \int f_{\text{ex}}(\rho, \vec{r}) \rho(\vec{r}) d\vec{r}.$$

The proportionality factor of 1/2 avoids double counting of contacts.

The mean-field approximation replaces the local density $\rho(\vec{r})$ with the average pile density $\bar{\rho}$; the remaining integral over the excluded orientations can then be identified with the average excluded volume v_{ex} , defined [19] as the volume denied to particle j by the condition that it not overlap with particle i . The average contact number then scales linearly with packing concentrations and the number density of a pile is

$$\rho = \frac{2\langle c \rangle}{v_{\text{ex}}}.$$

The excluded volume for cylinders of length L and thickness D is [19]

$$\begin{aligned} v_{\text{ex}} &= (\pi/2)L^2d + \frac{\pi(\pi+3)}{4}Ld^2 + (\pi^2/8)d^3 \\ &= L^3 \left[\frac{\pi}{2}\alpha + \frac{\pi(\pi+3)}{4}\alpha^2 + (\pi^2/8)\alpha^3 \right]. \end{aligned}$$

and, since the particle volume is $v_p = (\pi/4)d^2L$ and $\phi = \rho v_p$, the packing fraction is

$$\phi = \frac{2\langle c \rangle(\pi/4)d^2L}{L^3 \left[(\pi/2)\alpha + \frac{\pi(\pi+3)}{4}\alpha^2 + (\pi^2/8)\alpha^3 \right]} \quad (1)$$

$$= \frac{4\pi\langle c \rangle\alpha}{4\pi + 2\pi(\pi+3)\alpha + \pi^2\alpha^2}. \quad (2)$$

The predicted packing fraction $\phi(\alpha)$ has one single free parameter, the average contact number $\langle c \rangle$. We (and others [18]) noticed that significant orientational order exists when the cylinder diameter D is less than 1 particle length L . This violates the main assumption of the model, and so we should not expect good agreement in this region. We therefore attempt to fit the prediction from Eq. 2 with all data taken in cylinders where $D/L > 1$. The resulting line is shown in Fig. 1. For large aspect ratios Eq. 2 reduces to $\phi \sim \langle c \rangle/\alpha$, a scaling that was noticed previously in 2-[9] and 3-dimensions [10]. The curvature in the data in Fig. 1 shows that this simple limit does not apply; the full expression of Eq. 2 (solid line) agrees quite well with the data. From the fit we find $\langle c \rangle = 5.25 \pm 0.03$, which agrees (within reported error) with the data reported by Philipse [10]. The constant contact number implies a significant screening effect, since the contact number could in principle scale

with aspect ratio. A similar result for two dimensional piles was found in earlier simulations[9].

The good agreement between experiment and a model that assumes an isotropic distribution of particle angle supports the claim that particles are initially randomly oriented. The discrepancy at small container size is understandable, as the orientational correlation induced by the narrow cylinder violates the fundamental assumption of the RCM.

III. FORCE SCALING IN DIFFERENT REGIONS

When the particle aspect ratio is low, the pile responds with local rearrangements and the drag force on an intruding object has a random-sawtooth appearance (Fig. 2(top)). The force increases linearly, indicating that the ball is at rest, before rapidly decreasing, indicating a burst of motion. The ball is brought to rest and the cycle repeats. Throughout the experiment, the bulk pile is at rest. While individual particles near the ball are moving, there is no collective pile motion. As the aspect ratio is increased, however, the pile exhibits a qualitative change to solid-like behavior. With the exception of a few stray particles, all particles are lifted upward, with no observed relative motion between particles. The resulting force vs. time diagram is shown in Fig. 2(bottom). Forces are normalized by the total pile weight, and so Fig. 2 shows that the force required to move the pile can be many times the actual pile weight. This is a consequence of force chains [7, 8] that terminate on the container walls. The ball is pushing upward on the particles, but the lateral deflections of the force chains translate this into a force normal to container walls. This normal force can be quite large, resulting in large frictional forces between the walls and the pile.

For intermediate aspect ratios, the pile displays characteristics of both the granular and solid states. Figure 2(middle) shows data from one such run. The pile first behaves much like that of smaller aspect ratio particles, although a close examination of the force (inset in Fig. 2(middle)) reveals small plateaus indicating small amounts of solid-body behavior. Then, with the ball in the middle of the pile, the entire pile jams and all particles above the ball are lifted. Corresponding to the plateaus in the force is the collective motion of the entire pile. The pile is visually observed to move as a solid body for a brief period of time. The breakup of the solid state is brought about by a collapse of the particles around the ball. As the pile is constantly rubbed against the sidewall (and, indeed, shows force fluctuations characteristic of dry friction) the length of time spent in the solid state is some indication of the pile's stability.

A Fourier transform of the force vs. time data in the granular and solid regions (Fig. 3) shows that both spectra show power law tails, albeit with different exponents indicating a different fluctuation origin. Data from the

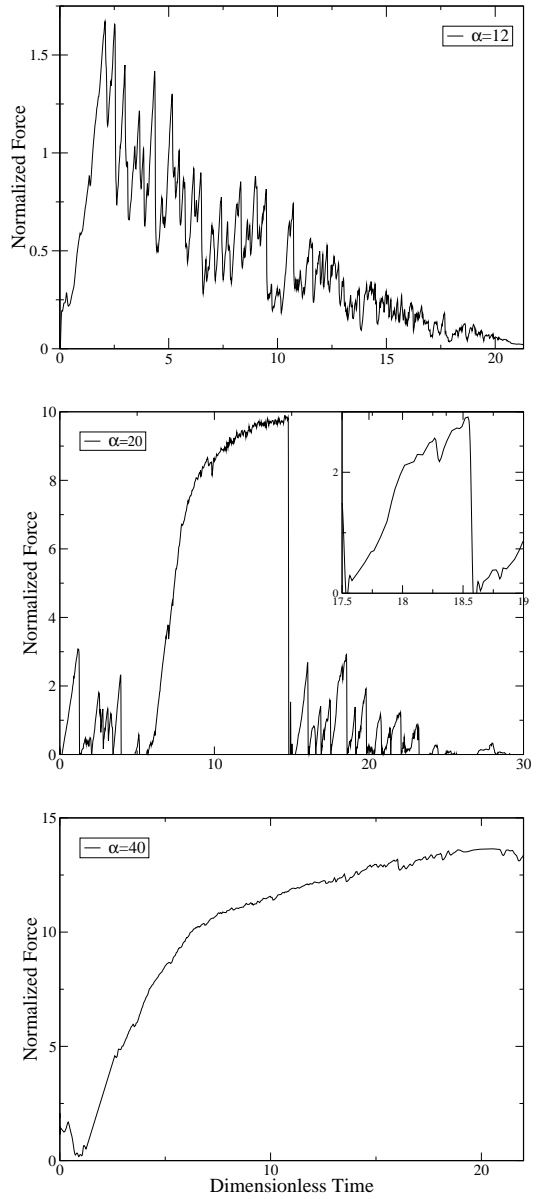


FIG. 2: Force vs. time data for a ball dragged through a pile of rods of aspect ratio 12 (top), 20 (middle), and 40 (bottom), all in a 2" tube. The low aspect ratio particles show the stick-slip behavior common in ordinary granular materials. The large aspect-ratio particles, however, act as a single solid body, with small fluctuations characteristic of dry friction. Intermediate aspect ratios show both behaviors in a single experiment on both large and small (inset) time scales.

granular region decay as $P(f) \sim f^{-2}$, consistent with earlier experiments on granular materials [20, 21]. Coupled with the visual observation of no macroscopic pile motion, this supports connecting the force serrations with local particle rearrangements. The forces in the solid region, however, decay as $P(f) \sim f^{-1}$. This is consistent with experimental work on dry friction [22], and so we infer that the pile is not moving steadily upward, but in

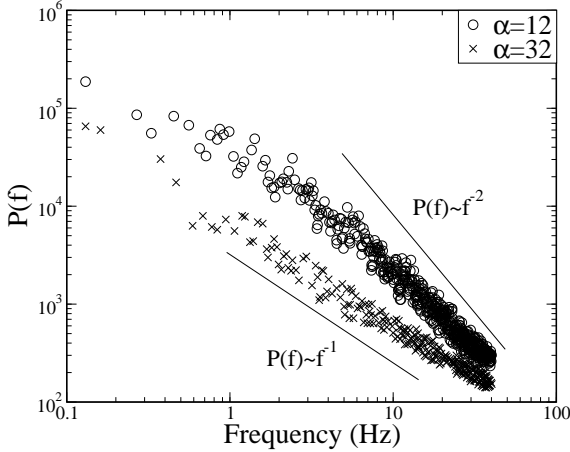


FIG. 3: Power spectra for force fluctuations from piles exhibiting granular (○) and solid (x) behavior. Both show power law tails, with the different exponents indicating a different mechanism for the fluctuations. The $1/f$ and $1/f^2$ decay are consistent with previous work on, respectively, dry friction and localized granular rearrangements. Both data sets taken in a $D=2$ ” diameter tube.

fact sticking on the side walls.

The exponent of the spectrum tail is a reliable indicator of the pile’s behavior. Shown in Fig. 4 is the exponent magnitude $|\beta|$ as a function of normalized tube diameter \tilde{D} . The data are grouped in three sets corresponding to the three different behaviors: stick-slip (○), transition (◊), and solid-like (□). Lying off the graph’s scale are three additional stick-slip data points (each representing an average of several runs) at $\tilde{D} = 5, 8, \& 12$; all are characterized by an exponent of magnitude of just under 2 with relatively small uncertainties. Data exhibiting transitional behavior show much larger uncertainties, indicating the statistically fluctuating nature of the behavior. While all force spectra from these experiments show the plateaus characteristic of the transition region, the relative amount of time spent on a plateau (as opposed to stick-slip) varies wildly from run to run. Data in the solid region have exponents close to one with small uncertainties (with the exception of data at $\tilde{D} = 1.2$, which we suspect was very close to the transition region).

IV. DYNAMIC PHASE DIAGRAM

To better understand the transition from granular to solid-like motion, we have mapped out the dynamic phase diagram of the behavior as a function of the two control parameters — aspect ratio α and container diameter \tilde{D} . It is in fact more revealing to use the inverse container diameter $1/\tilde{D}$. This is because when the particle length is increased but tube diameter held fixed both the aspect ratio and inverse diameter ($\delta \equiv L/D$) increase linearly, and so a sequence of experiments in which particle length

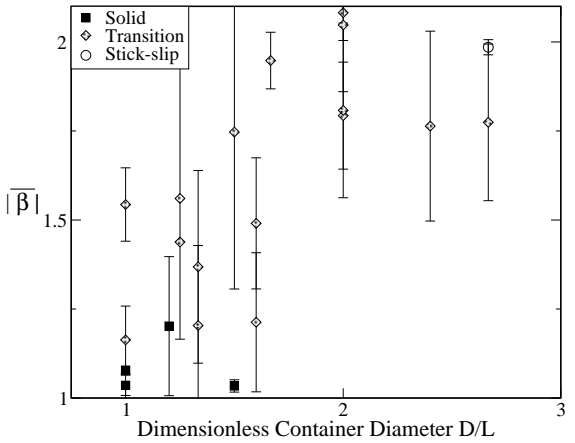


FIG. 4: Exponents of the spectra tails for experimental runs of varying aspect ratios plotted vs. normalized container diameter $\tilde{D} = D/L$. Filled symbols are aspect ratios larger than 20, which display solid-like motion in containers less than 1.5 particle lengths across.

is increased shows up as straight lines in $\delta - \alpha$ space. This is shown in Fig. 5.

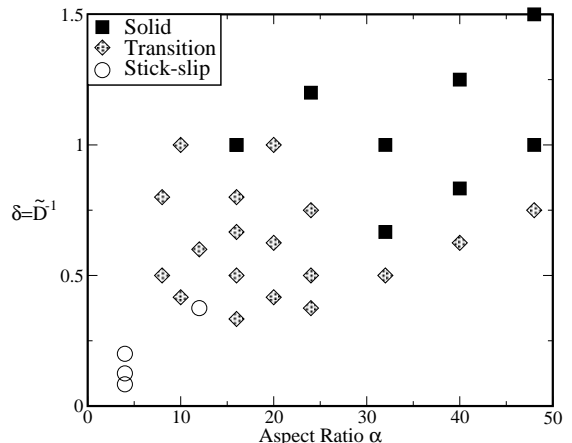


FIG. 5: Phases exhibited by granular piles as a function of two control parameters — the aspect ratio α and the inverse container diameter $\delta \equiv \tilde{D}^{-1}$. Smaller aspect ratio particles show the stick-slip behavior of granular materials, while larger aspect ratio particles act as a solid body when the container is small enough.

As one would expect, when the aspect ratio is very small, the pile behaves in a canonically granular manner. Nevertheless, the signature characteristics of the transition region — plateaus in the force data and a visual observation of collective motion — are seen in particles with aspect ratios as low as 8 when confined to cylinders whose diameter is twice the particle length. As the container diameter is further reduced, and the ability of particles to move around one another further constrained,

we expect solid-body motion to occur even for the small aspect ratios (upper left corner of the phase diagram), but we did not explore this region.

We did not investigate the dependence of the transition region on pulling speed. There are two different mechanisms through which the pulling speed can become significant: elastic unloading (particularly significant in a stiff machine) and particle rearrangements. We show here that we are well below the critical velocities at which either of these become important. In a theoretical investigation of frictional disks pushed upward through a vertical pipe, Bratberg et al.[17] found a transition that depended on the relative value of two time scales, $t_k = (\frac{m}{k})^{1/2}$ (m the pile weight, k the spring constant of the pulling mechanism) corresponding to the elastic unloading and $t_g = \frac{v}{g}$ the time for a particle to accelerate due to gravity to velocity v . An order-of-magnitude estimation of these values for our system is $m \approx 1$ kg, $v = 0.01$ m/s, and $k = 1600$ N/m, and therefore

$$\frac{t_k}{t_g} = \frac{\sqrt{\frac{m}{k}}}{v/g} \approx \frac{10^{-2}}{10^{-3}} \text{ s} \approx 10.$$

Using these numbers, we would expect a significant influence of pushing velocity to occur at a characteristic velocity of about $v_c = \sqrt{\frac{m}{k}}g \approx 24$ cm/s, twenty times our actual pulling speed. Therefore, our pulling “spring” is soft enough, and our velocities slow enough, so that the drop in force is not significant.

If the particle rearrangements are governed solely by gravitational forces, then the ratio of the time it takes a particle to fall under gravity a distance equal to its length L $t_r = \sqrt{\frac{L}{g}}$ to the time it takes the intruder to move that distance $t_i = L/v$ is important. The ratio of these times, using our approximate parameters, is then

$$\frac{t_i}{t_r} = \frac{\sqrt{gL}}{v} \approx 50,$$

leading to a critical velocity of $v_c = \sqrt{gL} \approx 50$ cm/s, about 50 times faster than the current pulling speed. Thus, the intruder moves a negligible distance while the grains themselves are re-orienting. The above analyses imply that we are in the quasi-static region of behavior and will not see significant changes in the behavior unless the pulling speed is increased by at least an order of magnitude.

Philipse observed that particles with aspect ratios larger than 35 did not flow when poured from a bucket, but rather emerged as a single, solid plug. The explanation given was a geometric entanglement of the rods.

Interestingly, however, we do not observe the solid behavior in particles with an aspect ratio of 48 when poured into the large cylinder. It may be that, in response to the localized disturbance of a small intruder, the pile can make small rearrangements necessary to allow the intruder to pass through while still maintaining an overall rigid structure. An important next step in this work will be to investigate the effect of intruder size on phase behavior. For small intruders, we imagine we are probing details of the spaces (voids) in the pile while larger intruders probe the pile’s rigidity. This would imply a critical length scale related to particle length and width, consistent with our observation that the particle aspect ratio alone does not completely determine the pile’s behavior.

V. CONCLUSIONS

We have observed three qualitatively different types of behavior in large aspect-ratio granular materials in response to a local disturbance: canonically granular stick-slip, solid-body like motion, and a transition region that is a combination of the two. The phase space of this behavior has been mapped out as a function of two control parameters, the particle aspect ratio and container diameter. We have found that even low aspect-ratio particles can exhibit temporary solid-body motion that is characteristic of transitional behavior. Surprisingly, the larger aspect ratio particles do not behave as solid bodies when the container is large enough. The granular and solid states both show force fluctuations with spectra that have power-law tails, although the exponents are characteristically different.

We have also investigated the packing fraction as a function of these two control parameters. While there is a slight dependence on container size, we find a distinct dependence on aspect ratio that agrees quite well with the mean-field Random Contact Model. This is perhaps surprising, as we observe some orientational ordering that violates a main assumption of this model.

Acknowledgments

This research was supported by an award from the Research Corporations; Scott Franklin is a Cottrell Scholar of Research Corporation. Acknowledgment is also made to the Donors of the American Chemical Society Petroleum Research Fund for support of this research.

[1] K. To, P.-Y. Lai, and H. K. Pak, *Phys. Rev. Lett.* **86** (2001).
[2] K. To, P.-Y. Lai, and H. K. Pak, *Physica A* **315** (2002).

[3] K. To and P.-Y. Lai, *Phys. Review E* **66** (2002).
[4] I. Zuriguel, A. Garcimartin, D. Maza, L. A. Pugnaloni, and J. M. Pastor, *Physical Review E* **71** (2005).

- [5] R. Albert, M. A. Pfeifer, A. L. Barabasi, and P. Schiffer, Phys. Rev. Lett. **82** (1999).
- [6] I. Albert, P. Tegzes, R. Albert, J. G. Sample, M. A. Pfeifer, A. L. Barabasi, and P. Schiffer, Phys. Rev. Lett. **84** (2000).
- [7] C. S. O'Hern, S. A. Langner, A. J. Liu, and S. R. Nagel, Phys. Rev. Lett. **86** (2001).
- [8] S. N. Coppersmith, C. H. Liu, S. Majumdar, O. Narayan, and T. A. Witten, Phys. Rev. E **53** (1996).
- [9] K. Stokely, A. Diacou, and S. V. Franklin, Physical Review E **67** (2003).
- [10] A. Philipse, Langmuir **12** (1996).
- [11] F. Zhou, S. G. Advani, and E. D. Wetzel, Physical Review E **69** (2004).
- [12] F. Zhou, S. G. Advani, and E. D. Wetzel, Physical Review E **71** (2005).
- [13] J. Geng and R. P. Behringer, Physical Review E **71** (2005).
- [14] G. Hill, S. Yeung, and S. A. Koehler, Europhysics Letters **72** (2005).
- [15] M. B. Stone, R. Barry, D. P. Bernstein, M. D. Pelc, Y. K. Tsui, and P. Schiffer, Physical Review E **70** (2004).
- [16] M. B. Stone, D. P. Bernstein, R. Barry, M. D. Pelc, Y. K. Tsui, , and P. Schiffer, Nature **427** (2004).
- [17] I. Bratberg, F. Radjai, and A. Hansen, Physical Review E **71** (2005).
- [18] G. Lumay and N. Vandewalle, Physical Review E **70** (2004).
- [19] L. Onsager, Ann. N.Y. Acad. Sci. **51** (1949).
- [20] I. Albert, P. Tegzes, R. Albert, J. G. Sample, A. L. Barabasi, T. Vicsek, B. Hang, and P. Schiffer, Phys. Rev. E **64** (2001).
- [21] B. Miller, C. O'Hern, and R. P. Behringer, Phys. Rev. Lett. **77** (1996).
- [22] H. J. S. Feder and J. Feder, Phys. Rev. Letters **66** (1991).